Archives of the Balkan Medical Union
vol. 61, no. 3, pp. 336-351
September 2026
Copyright © 2026 Balkan Medical Union

ORIGINAL PAPER

MORPHOLOGY OF FIBRIN-BONE SCAFFOLD OBTAINED BY SIMULTANEOUS CENTRIFUGATION OF BLOOD WITH BONE MATRIX

Anton I. CHELIY[1], Andrii V. PANTUS[2]✉, Mykola M. ROZHKO[1], Iryna R. YARMOSHUK[1], Nataliia Ye. KOVALCHUK[3]

[1] Department of Dentistry, Institute of Postgraduate Education, Ivano-Frankivsk National Medical University, Ivano-Frankivsk, Ukraine
[2] Department of Surgical Dentistry, Ivano-Frankivsk National Medical University, Ivano-Frankivsk, Ukraine
[3] Department of Histology, Cytology and Embryology, Ivano-Frankivsk National Medical University, Ivano-Frankivsk, Ukraine

Received 29th May 2026, Accepted 18th Aug 2026
https://doi.org/10.31688/ABMU.2026.61.3.01

Abstract

Introduction. Current platelet-rich fibrin technologies used for bone regeneration typically involve either mechanically less stable fibrin-bone scaffolds with improved inductive properties or more stable fibrin scaffolds that are difficult to fully integrate with the bone matrix. Finding the optimal balance between scaffold stability and improving its inductive properties remains a priority for regenerative medicine.
The aim of the study was to investigate the structure of the fibrin scaffold on the surface of the bone matrix and to determine the effect of different centrifugation regimes on the formation of a biologically active scaffold.
Materials and methods. Electron microscopic and histological studies were performed on fibrin-bone matrices obtained using different centrifugation modes of human blood.
Results. Modification of allogeneic material leads to the formation of a well-developed fibrin network with

Résumé

Morphologie d'un échafaudage fibrine-os obtenu par centrifugation simultanée de sang et de matrice osseuse

Introduction. Les technologies actuelles de fibrine riche en plaquettes utilisées pour la régénération osseuse font généralement appel soit à des matrices fibrine-os mécaniquement moins stables mais aux propriétés inductives améliorées, soit à des matrices de fibrine plus stables mais difficiles à intégrer pleinement à la matrice osseuse. Trouver le juste équilibre entre la stabilité de la matrice et l'amélioration de ses propriétés inductives demeure une priorité en médecine régénérative.
L'objectif de cette étude était d'étudier la structure de la matrice de fibrine à la surface de la matrice osseuse et de déterminer l'effet de différents régimes de centrifugation sur la formation d'une matrice biologiquement active.

✉ Address for correspondence: Andrii V. PANTUS
Department of Surgical Dentistry, Ivano-Frankivsk National Medical University, Ivano-Frankivsk, Ukraine
Address: Galitska str. 2, Ivano-Frankivsk, 76000 Ukraine
E-mail: kovalchuk-natalja@ukr.net

a high concentration of platelets, accompanied by an increase in surface roughness and porosity. This was confirmed by the peculiarity of the nanofibrous structure of the fibrin mesh, which is present not only on the surface of the porous structure of the bone matrix, but also inside its small micropores. Thus, compared to existing methods, experimental centrifugation protocols showed a combined fibrin matrix structure that combined coarser nanofibers with a fine dense mesh, with a higher number of platelets and macrophages.
Conclusion. The experimental two-stage centrifugation regimen combines mechanical stability, due to the organized fibrous structure of fibrin, with inductive properties, due to the high concentration of growth factors and a greater number of cells in the resulting scaffold.

Keywords: bone matrix, platelet-rich fibrin, scanning electron microscopy, osteoconduction, osteoinduction.

List of abbreviations:
SEM – scanning electron microscopy
PRF – platelet-rich fibrin
VEGF-A – vascular endothelial growth factor
PDGF-AA – platelet-derived growth factor

Matériels et méthodes. Des études de microscopie électronique et d'histologie ont été réalisées sur des matrices fibrine-os obtenues par différents modes de centrifugation de sang humain.
Résultats. La modification du matériau allogénique conduit à la formation d'un réseau de fibrine bien développé, riche en plaquettes, et s'accompagne d'une augmentation de la rugosité et de la porosité de surface. Ceci a été confirmé par la particularité de la structure nanofibreuse du réseau de fibrine, présente non seulement à la surface de la structure poreuse de la matrice osseuse, mais aussi à l'intérieur de ses micropores. Ainsi, comparativement aux méthodes existantes, les protocoles de centrifugation expérimentaux ont révélé une structure matricielle de fibrine combinant des nanofibres plus grossières à un réseau fin et dense, avec un nombre plus élevé de plaquettes et de macrophages.
Conclusion. Le protocole expérimental de centrifugation en deux étapes allie stabilité mécanique, grâce à la structure fibreuse organisée de la fibrine, et propriétés inductives, dues à la forte concentration de facteurs de croissance et au nombre accru de cellules dans l'échafaudage obtenu.

Mots-clés: matrice osseuse, fibrine riche en plaquettes, microscopie électronique à balayage, ostéoconduction, ostéoinduction.

Introduction

Despite the experience with the clinical use of bone grafting materials and the availability of a sufficient amount of approved products[1-5], the search for ways to further improve their efficacy, safety and reliability continues. One such approach to enhancing the osseointegration characteristics of these materials involves physicochemical modification of the bone matrix by altering its surface porosity. This process ensures an optimal adhesion of the cellular-fibrous material to the surface of such biomaterials during osteoconduction in the tissue while wound healing and osteograft engraftment. In earlier studies[2,3], this method of modifying bone-plastic materials received extensive coverage and approval of transplantation results; however, the mechanisms of osteoconduction of modified bone materials remain insufficiently studied. In addition to modifying the surface of the materials themselves, another pressing issue is the creation of a unique inductive environment to stimulate the regeneration of surrounding tissues. One such environment is platelet-rich fibrin (PRF), which is the most widely used in medicine and dentistry. This material, derived from the patient's own blood, has several significant advantages, including enhanced protein release, expression of growth factors, stimulation of fibroblast proliferation, and others[6-10]. Current methods indicate that the combination of bone-plastic material is predominantly achieved using injectable forms of PRF[11]. This approach relies on a liquid-consistency, plasma-enriched solution in which, although it is possible to fully mix the material granules, such a matrix will not be mechanically stable.

In contrast, other methods allow to produce stronger fibrin scaffolds, such as A-PRF or L-PRF. In particular, De Almeida et al. analyzed the tensile strength of such fibrin matrices[12,13].(ref 13 seems to be NOT related to De Almeida) However, despite their good mechanical properties, it is not possible to integrate bone-plastic material granules into this type of gel-like PRF.

In our opinion, the combination of a bone-plastic matrix with a mechanically stable fibrin PRF will ensure the stability of such a scaffold during the sinus lift technique. Furthermore, due to the presence of growth factors, it will stimulate bone tissue regeneration.

The aim of the study was to investigate the structure of the fibrin scaffold on the surface of the bone matrix and to determine the effect of different

centrifugation regimes on the formation of a biologically active scaffold.

Materials and methods

Morphometric and enzyme-linked immunosorbent assay (ELISA) analyses of fibrin matrix samples and plasma fluid were performed at the Ivano-Frankivsk National Medical University, Ukraine, from 2023 to 2025. Scanning electron microscopy of fibrin-bone matrix samples was performed at Ivan Franko National University of Lviv, Ukraine. All samples for the study were obtained by centrifugation of venous blood (n=60) from patients aged 30 to 45 years, as part of planned jaw bone augmentation surgeries using PRF, which were performed at the Ivano-Frankivsk National Medical University. The patients' venous blood was collected in the morning at the same time of day, immediately before the planned surgery. All patients were practically healthy, without any bad habits or concomitant pathology, in particular without any pathological condition of bone tissue, oral mucosa, or general somatic diseases. The exclusion criteria were pregnancy and patients taking medications that could directly or indirectly affect blood clotting processes, its cellular composition, and biochemical properties.

The study was performed in accordance with the principles of the Helsinki Declaration on the Protection of Human Rights, the Council of Europe Convention on Human Rights and Biomedicine. The study protocol was approved by the Local Ethics Committee of Ivano-Frankivsk National Medical University (protocol no. 138/23, dated 24.10.2023). Written informed consent was obtained for the study, as well as for the collection and processing of patients' data. Fibrin-platelet concentrates, namely L-PRF, A-PRF, I-PRF, Sticky Bone, were prepared according to the standard protocol for the preparation of PRF concentrates. The experimental centrifugation regimes developed by the authors included 2500 rpm (12 minutes), 3000 rpm (3 minutes) (Experimental A) and 2000 rpm (12 minutes), 2500 rpm (3 minutes) (Experimental B) (these experimental centrifugation regimes are detailed in Patent N° 156181, published 22.05.2024). The centrifugation speed and time were calculated based on the radius of the centrifuge rotor and derived directly from the g-index (relative centrifugal force – RCF). The fibrin-bone scaffold was prepared by simultaneous centrifugation of the bone-plastic material and bone tissue. Such matrices were prepared according to a protocol developed by the authors, which included extraction of blood into a vacuum tube, placing a filter that was developed by the authors and composed of biocompatible titanium Ti-6Al-4V (Patent N° 152966, published 03.05.2023), in conjunction with the bone-plastic material (Fig. 1).

The fibrin matrix and fibrin-bone scaffold fragments, measuring 1×1 mm and prepared using the method described above, were fixed in a 2.4% glutaraldehyde solution in phosphate buffer (pH=7.4) for 24 hours at 4°C, after which they were passed through a series of alcohols of increasing concentration (50- 96 abs. ethanol). The fragments were then freeze-dried using the critical point bypass method in liquefied CO_2 in a Samdri-780A apparatus (USA) (Fig. 2).



a b

Fig. 1. General view of the fibrin-bone scaffold obtained by simultaneous centrifugation of the bone-plastic material granules and the patient's blood: a – appearance in the test tube immediately after centrifugation; b – preparation of the fibrin-bone scaffold for implantation into the bone defect.



Fig. 2. General view of the apparatus for drying using the method of avoiding critical point transition in a CO_2 environment.

The specimens were prepared with meticulous care and subsequently mounted on microscope slides using an electrically conductive adhesive, and then coated with a layer of chemically pure aluminum (999 grade) to ensure the electrical conductivity of the entire micro-specimen. The prepared specimens were analyzed using a JEOL-25M-T220A scanning electron microscope (SEM) (Tokyo, Japan) with an accelerating voltage of 20-25 kV at various magnifications in the backscattered electron mode. The concentrations of the growth factors VEGF-A (Vascular Endothelial Cell Growth Factor) and PDGF-AA (Platelet-Derived Growth Factor) were determined in fractions obtained under various centrifugation conditions: L-PRF, A-PRF, I-PRF, Sticky Bone, in accordance with the standard protocol and the Experimental A and Experimental B protocols developed by the authors. The liquid plasma fraction obtained by squeezing from the fibrin clot was then subjected to an enzyme-linked immunosorbent assay (ELISA), a process which was performed according to the standard protocol as per the instructions using an ELISA kit. The optical density (OD) of each well was determined at a wavelength of 450 nm using an ER500 microplate reader.

Since the mechanical stability of the fibrin-bone scaffold is influenced not only by the structure of the fibrin fibers but also by their quantity, the ratio of the liquid plasma fraction to the gel-like fibrin was determined based on the following criteria: the volume of the liquid plasma fraction (mL) (determined by collecting the liquid plasma fraction immediately after centrifugation), volume of the gel-like fraction (cm^3) (determined in a test tube immediately after centrifugation), the volume of the liquid fraction of the pressed portion (mL) (determined by collecting the liquid plasma fraction obtained immediately after pressing the gel-like fraction), followed by the determination of the area (mm^2) of the pressed polymerized fibrin clot. The analysis of this ratio was performed based on a determined standard 8 mL of blood volume and considering the six main centrifugation modes we have selected, without the addition of bone-plastic material granules. To count the amount of cells in the fibrin matrix, the histological examination of the fibrin preparations was additionally performed. For this purpose, following centrifugation, the fibrin matrix was placed in a 10% solution of neutral formalin (pH 7.0), followed by dehydration in a series of ascending alcohols, toluene, and a toluene-paraffin mixture (1:1), and paraffin (at 37°C). Serial paraffin sections measuring 4–6 μm in thickness were prepared using a sliding microtome. The histological sections of the fibrin matrix were stained using standard methods, namely with hematoxylin and eosin, and according to the Mason and Romanovsky-Giemsa methods.

The statistical analysis of the numerical data was performed using Microsoft Excel 2019 software (Microsoft Office 2019 (Microsoft). All the quantitative data obtained in the study corresponded to the normal type of distribution according to the Shapiro-Wilk's W test, and therefore the interval (M±m) was used to represent their central tendency: arithmetic mean (mean) ± standard error. To assess the reliability of the observed differences in the results obtained in comparison with the control group, the parametric t-test (Student's test) was applied. The reliability of the difference in qualitative data between the comparison groups was determined according to the results of calculating the Chi-squared test with Yates's correction for continuity. A value of $p<0.05$ was considered to be probable.

Results

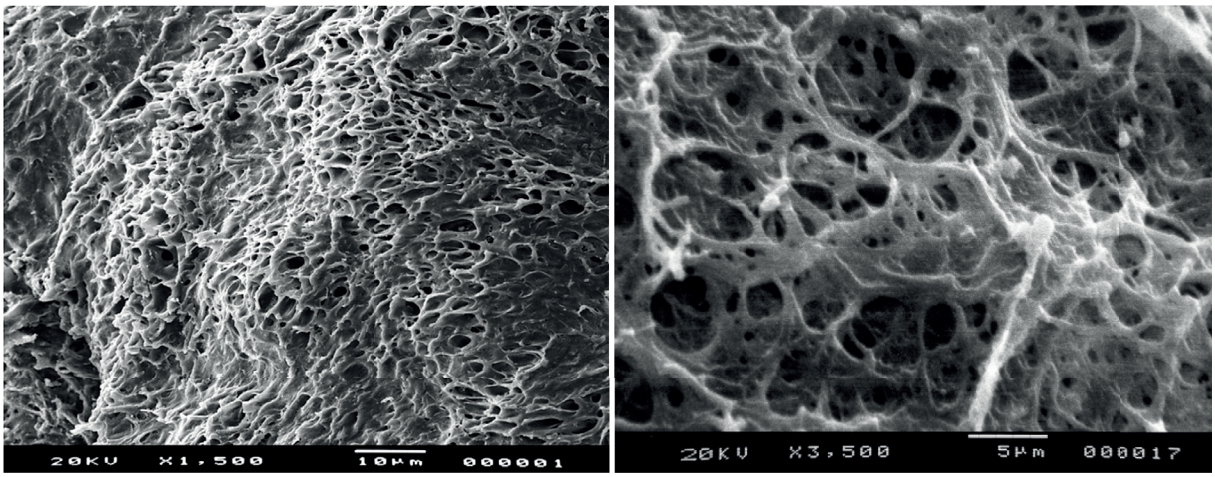
Prior to an analysis of the fibrin-bone scaffold, we have first determined the ratio of the liquid plasma fraction to the gel-like fibrin (Table 1).

The comparative analysis of the ratio of liquid plasma fraction to gel-like fraction demonstrated that the largest area of the resulting fibrin matrix was

Table 1. Comparative analysis of the ratio of the liquid plasma fraction to the gel-like polymerized fibrin fraction

Centrifugation modes	*Indices of the ratio of the liquid part of plasma to gel-like fibrin*			
	Volume of liquid plasma fraction (ml)	*Volume of gel-like plasma fraction (cm^3)*	*Pressed liquid plasma fraction (ml)*	*Clot parameters: area (mm^2)*
L-PRF control	1.42+0.032*†	2.62+0.042†	0.68+0.025*†	273.1+5.61*†
A-PRF control	1.54+0.040*†	2.42+0.033*†	0.42+0.026*†	264.5+4.99*
i-PRF control	2.62+0.029*†	2.70+0.042†	2.64+0.019*†	54.2+3.010*†
Sticky bone control	2.74+0.032*	2.52+0.063†	2.46+0.040*†	40.3+2.32*†
Experimental A	1.26+0.018*	2.60+0.052*	0.32+0.018*	322.4+8.28*
Experimental B	2.72+0.029*	1.82+0.068*	0.84+0.046*	242.9+11.33*

Notes: 1. * – p<0.05 when comparing the control and Experimental A blood fractions and between the Experimental A and Experimental B blood fractions.
2. † – p<0.05 when comparing the control and Experimental B blood fractions.



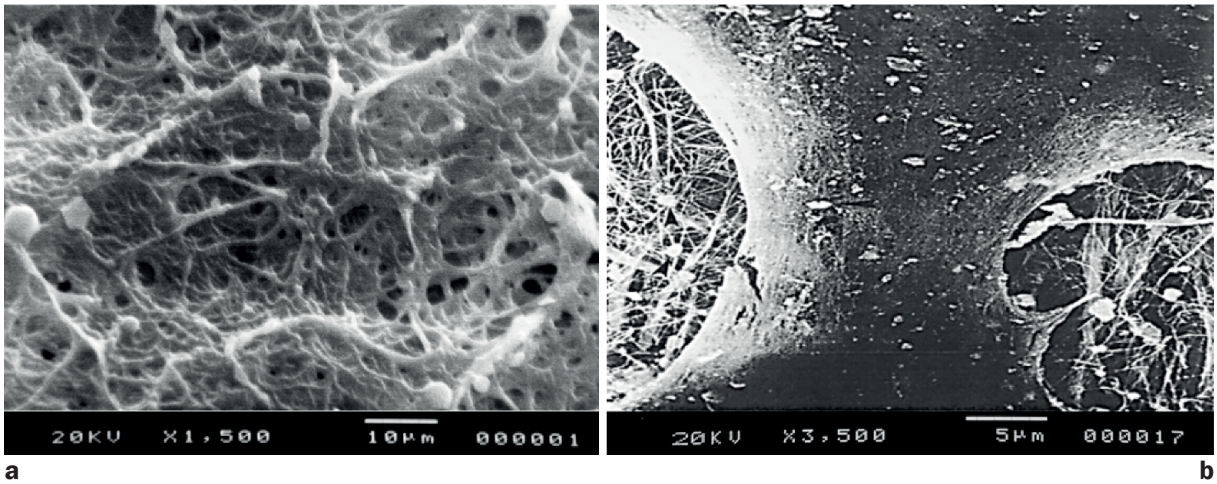
a b

Fig. 3. A general perspective of the surface of an allogeneic graft modified with autoplasma-enriched with platelet-rich plasma under centrifugation conditions Experimental A and Experimental B. Method: SEM; accelerating voltage 10 kV; original magnification: a×1,500, b×3,500; scale bar: a=10 µm, b=5 µm.

observed when using experimental protocols, particularly the Experimental A protocol. The largest amount of organized fibrin was also observed in the L-PRF, A-PRF, and Experimental B protocols, as evidenced by the indices of the pressed liquid fraction and the resulting fibrin area after pressing. The largest volume of the liquid plasma fraction included in the fibrin scaffold was observed in the I-PRF and Sticky Bone centrifugation protocols. In our opinion, the fact that the area of the resulting fibrin scaffold is 5-6 times smaller under these protocols indicates a significantly lower amount of polymerized fibrin, which directly affects the lower mechanical stability of such a scaffold compared to previous centrifugation modes. Despite the total volume of the gel-like fraction of blood plasma obtained under different centrifugation modes did not differ significantly from one another, the mechanical stability of the fibrin scaffold, particularly its tensile strength, can only be confirmed when using the Experimental A and Experimental B protocols, as well as the L-PRF and A-PRF protocols. The performed analysis of the effect of biocompatible titanium Ti-6Al-4V on fibrin scaffold formation revealed a statistically significant ($p<0.05$) decrease to 0.28±0.014 mL in the volume of the liquid plasma fraction formed immediately after centrifugation, accompanied by an increase in the area of the extruded fibrin scaffold up to 456±15.27 mm^2.

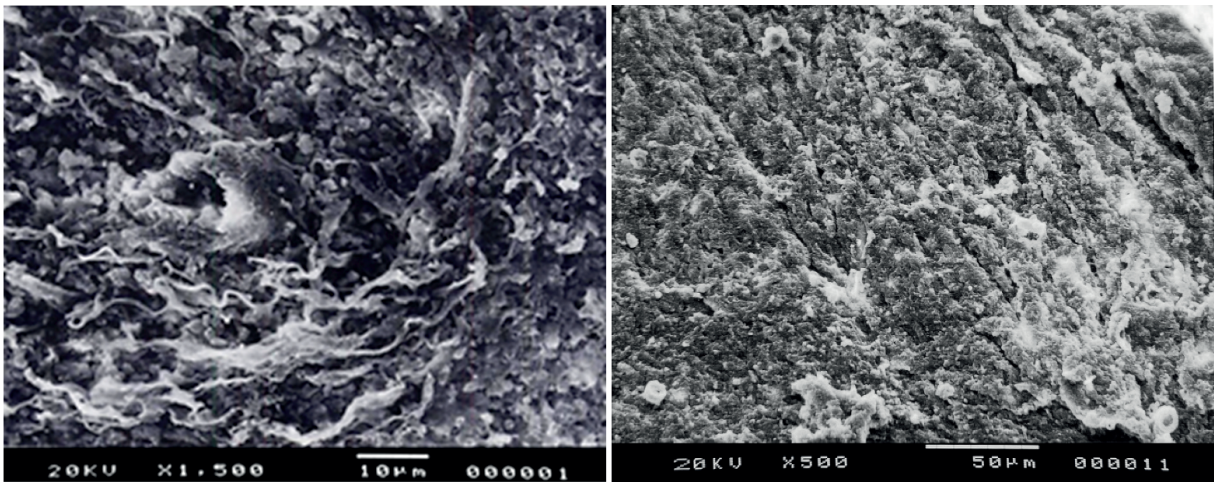
The surface of the bone-plastic material specimens treated with autoplasma-enriched with platelet-rich mass using the authors' method has exhibited a spongy, fine-mesh microstructure (Fig. 3). At high magnifications, an organized fibrin network is visualized within the microporous structure of the bone matrix during its simultaneous centrifugation with the patient's blood (Fig. 4).

SEM-images of the untreated bone graft surfaces used as controls revealed a smoother surface without the additional fibrillar reticular components observed in the method developed by the authors. Calcification deposits in such preparations not integrated with fibrin, in the form of particles or granules, were found



a b

Fig. 4. SEM micrograph of a biograft showing a densely organized fibrin network (a) with organized fibrin fibers within the micropores of the allogenic bone matrix (b) under centrifugation conditions Experimental A and Experimental B, together with bone-plastic material. Method: SEM; accelerating voltage 20 kV; original magnification: a×1,500, b×3,500; scale bar: a=10 µm, b=5 µm.



a b

Fig. 5. SEM-images of the surface of a xenomaterial showing distinct lamellar structures (a) and a fine-grained surface (b). Method: SEM; accelerating voltage 20 kV; original magnification: a×1,500, b×500; scale bar: a=10 µm, b=50 µm.

in large quantities on the surface of the preparation. At the same time, SEM-images consistently exhibited a fine-scale roughness and lamellar structure of the surface accompanied by wide flocs (Fig. 5a) in the calcified areas of the specimens (Fig. 5b).

Following the application of autoplasma enriched with platelet-rich plasma according to the I-PRF and Sticky Bone protocols, a slight difference in the surface structure of the matrix was observed in comparison to that of the previous preparations obtained using the two modes developed by the authors – Experimental A and Experimental B. Thus, in addition to platelet clusters, lamellar structures – flocs – were also detected (Fig. 6).

The significant calcification determined by us was clearly evident as raised plaques or nodules, small bright particles, or granules on the surface of the specimen (Fig. 7a). These features delineated irregular surface cavities associated with calcific deposits, which were frequently observed. It is noteworthy that SEM images revealed the presence of broad honeycomb-like structures, which were arranged in a planar pattern on the surface of the bone matrix. It is of particular importance that calcified deposits frequently accumulated in or around such surface voids (Fig. 7e).

During our study, we discovered that when the bone matrix and the patient's blood are subjected to simultaneous centrifugation, the formation of a nanofibrous fibrin structure occurs not only on the surface of the porous structure of the bone matrix but also within its fine micropores. This particular type of nano-assembly forms a continuous fibrin-bone scaffold, which is more stable in terms of its mechanical

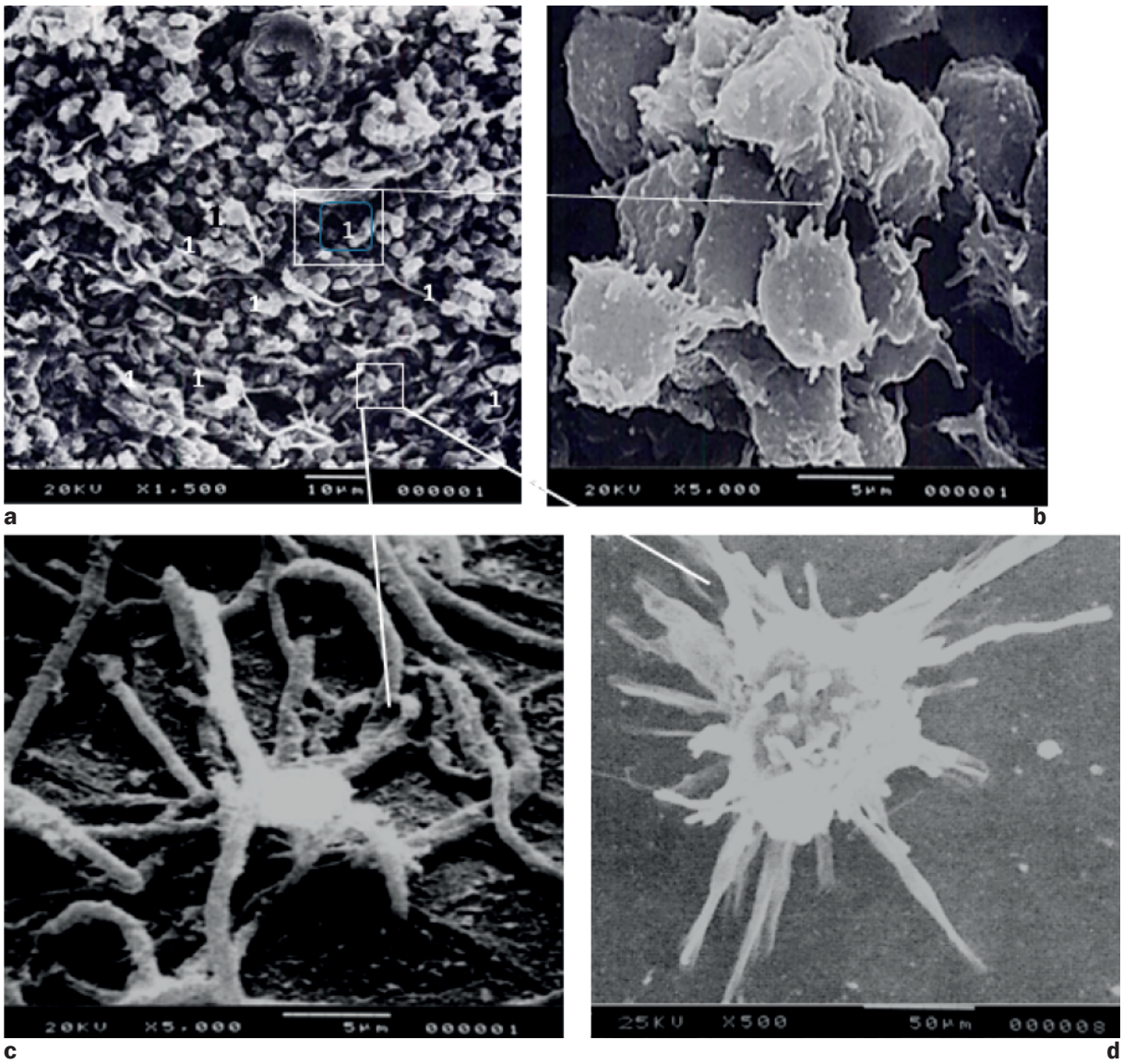


Fig. 6. SEM-image showing many fixed blood cells among lamellar structures – flocs (1) on the material surface after application of autoplasma enriched with platelet-rich mass obtained by centrifugation according to the I-PRF and Sticky Bone protocols (a) and individual activated platelets (b, c, d). Method: SEM; accelerating voltage 20 kV; original magnification: a×1,500, b and c×5,000, d×3,500; scale bar: a=10 µm, b and c=5 µm, d=50 µm.

properties than that produced by classical Sticky Bone protocols (Fig. 8).

It is precisely on such nanoporous surfaces that cells can attach after implantation, particularly osteoblasts derived from autologous bone, which initiate the process of graft osteoinduction with the participation of growth factors and neoangiogenesis from platelets.

It is also believed that a porous surface is one of the key factors contributing to the success of osteoconduction and osteointegration processes in the bone matrix. The method of combining autologous platelet-rich plasma with subsequent coating with a formed fibrin mesh is a type of substrate-based method. Therefore, it was performed an analysis of the porous structure of the matrix both before and after the formation of the fibrin mesh. This analysis revealed a significant difference, particularly regarding the honeycomb structure of the bone matrix, which had a significantly more porous and looser surface (Fig. 9a, b, and Fig. 11), especially when compared to bone not modified with fibrin. Concurrently, a certain difference in the fibrin modifications of various types of bone matrix surfaces was noted, which can be either smooth-and-rough with integrated fibrin fibers (Fig. 9a), or a surface with adhesion of a large number of cellular elements, in particular platelets, on the walls of a honeycomb-like fine-rugose structure (Fig. 9b), or the bone matrix is covered by a dense, organized fibrin network (Fig. 10 a, b, c), on the fibers of which fixed platelets are detected (Fig. 11 b).

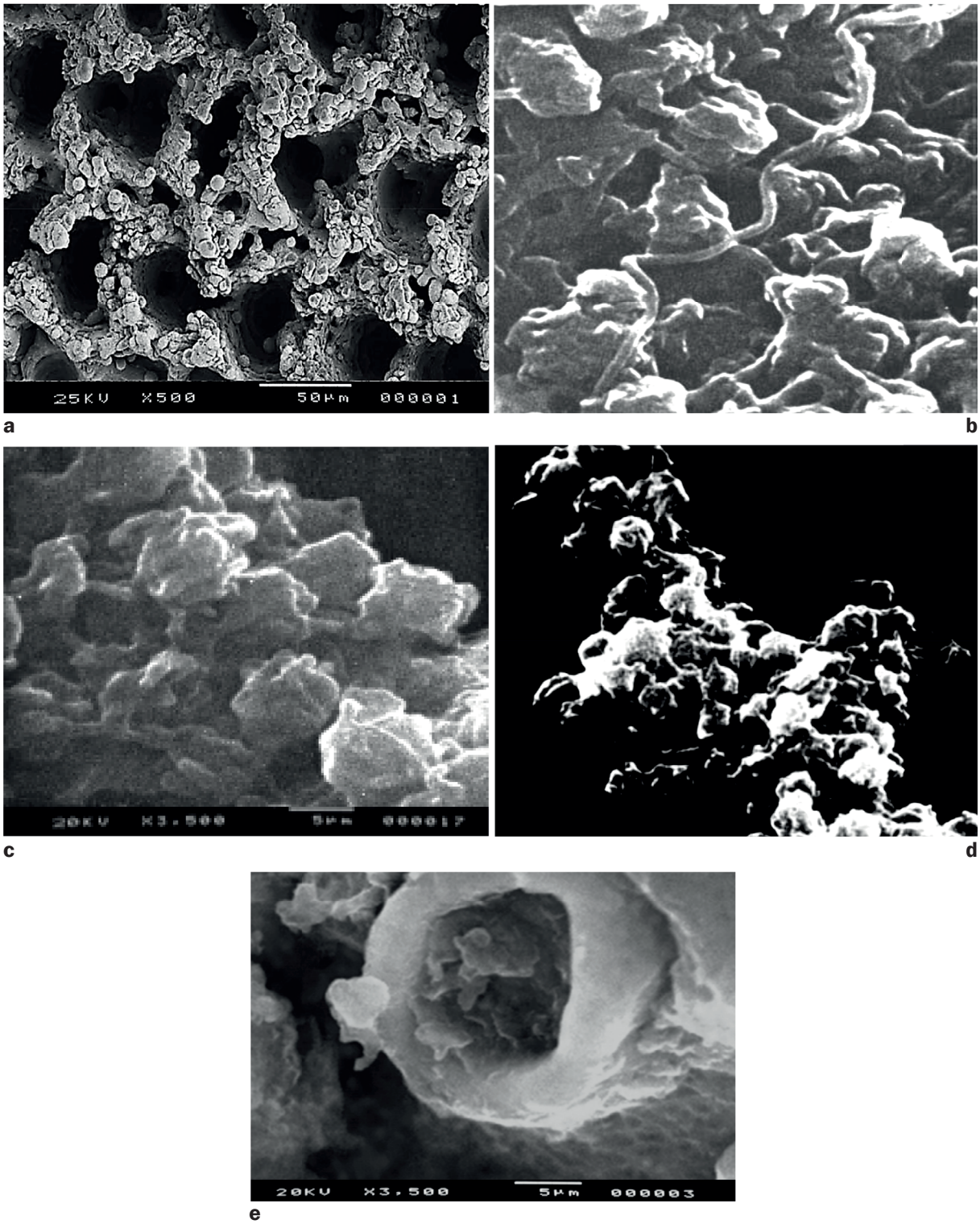


Fig. 7. SEM-image of the bone matrix surface obtained by means of simultaneous centrifugation of the bone matrix and the patient's blood. The presence of a large number of platelets (b) and mineralized material around the honeycomb-like pores should be noted (c, d). Method: SEM; a—accelerating voltage 25 kV, b—25 kV; original magnification: a ×500, b, c, e ×3,500; scale bar: a = 50 µm, b, c, e = 5 µm.

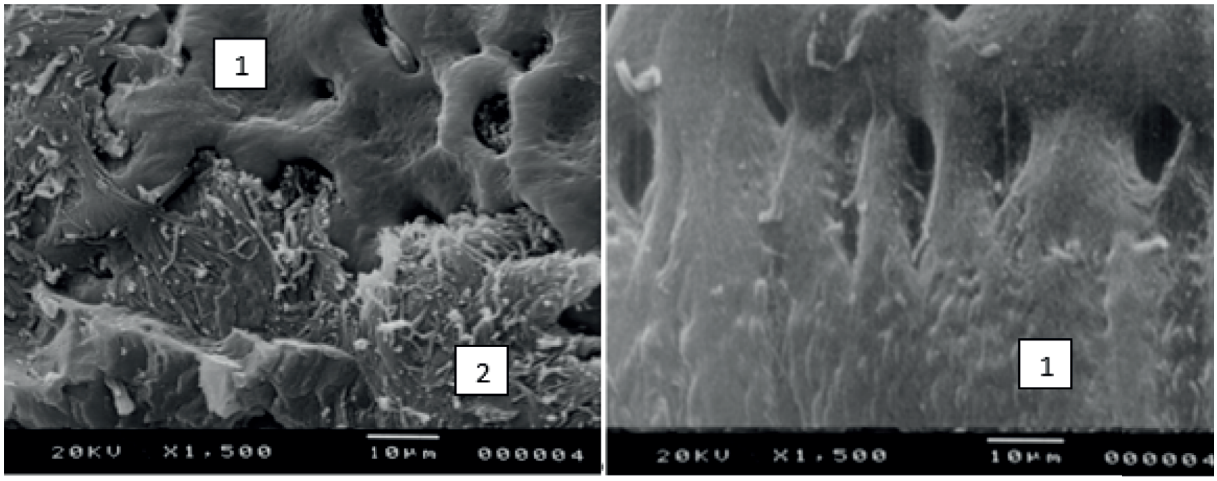


Fig. 8. SEM-micrograph showing the surface of the bone matrix (1). Note the presence of a fine fibrin network (2) embedded in the honeycomb-like openings and pores of the bone matrix (1) following simultaneous centrifugation of the patient's blood and bone according to the protocols. Method: SEM; accelerating voltage 20 kV; original magnification a, b×1,500 scale bar=10 µm, c×3,500 scale bar=5 µm.

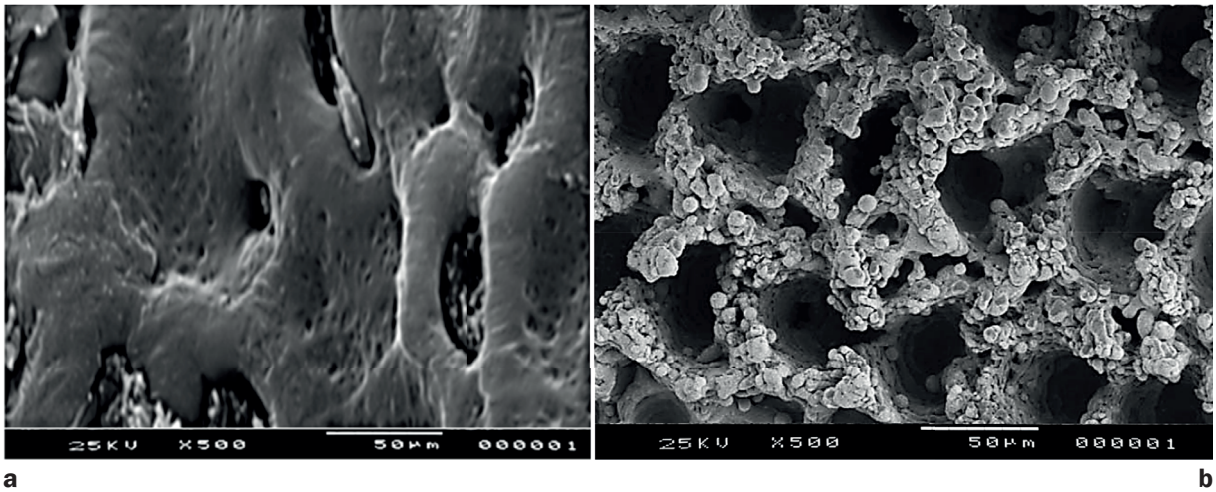


Fig. 9. SEM-images of fibrin-modified bone matrix surfaces with a smooth-rough surface and an integrated fibrin matrix (a) and a honeycomb-like fine-rough structure (b) obtained by the simultaneous centrifugation of the patient's bone and blood. Method: SEM; accelerating voltage 25 kV; original magnification: ×500; scale bar=50 µm.

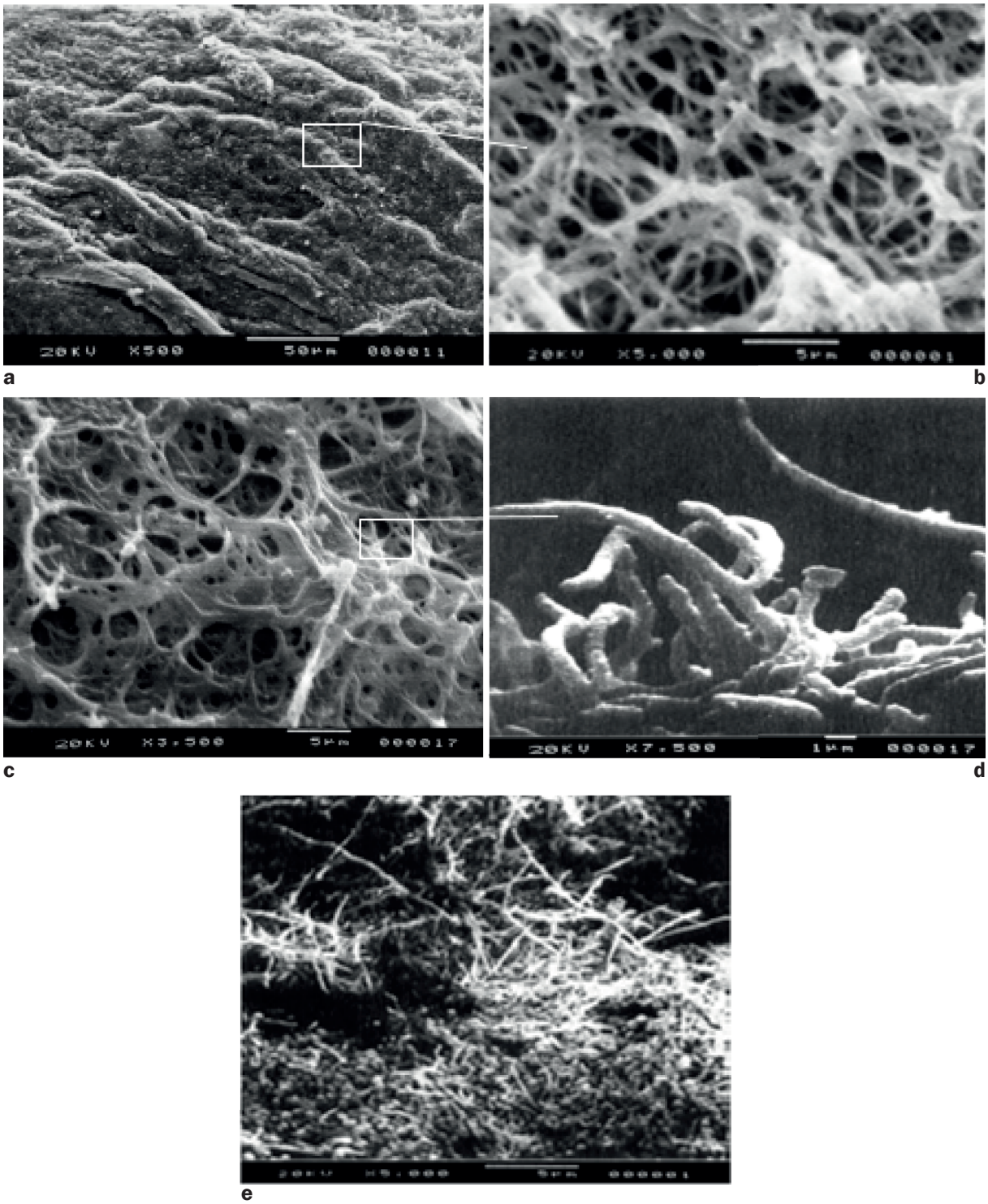


Fig. 10. SEM-images of the surface of the fibrin-bone matrix obtained by the simultaneously centrifuging the patient's bone and blood (a, b, c, d) and the use of the I-PRF and Sticky Bone protocols (e). Method: SEM; accelerating voltage 20 kV; original magnification: a×500, b, e×5,000, c×3,500, d×7,500; scale bar: a=50 µm, b, c, e=5 µm, d=1 µm.

An analysis of the structure of the fibrin-bone matrix shown in Fig. 10 reveals a significant difference between the organization of fibrin nanofibers themselves and the organized, dense network (Fig. 10 a, b, c, d) within the fibrin-bone scaffold obtained by simultaneous centrifugation of the patient's bone and blood, compared to the chaotic, loose structure resulting from plasma-based mixing using classical protocols (I-PRF and Sticky bone) (Fig. 10 e). Overall, the surface microtopography of the bone matrix after treatment with autologous plasma-enriched platelet-rich mass acquires a loose cellular structure

Table 2. Concentration of growth factors in blood plasma under different centrifugation conditions

Growth factors	*Protocols for the preparation of saturated platelet concentrates*					
	L-PRF control	*A-PRF control*	*I-PRF control*	*Sticky bone control*	*Experimental A*	*Experimental B*
VEGF-A pg/mL	48.96± 9.69*†	67.19± 14.14*†	117.95± 26.69	97.16± 13.00	109.22± 13.35	165.14± 42.06
PDGF-AA pg/mL	91.37± 0.57†	84.63± 4.51	71.51± 6.29	65.17± 4.55*	86.64±3.65	78.35±4.44

Notes: 1. * – $p<0.05$ when comparing the control and Experimental A blood fractions and the Experimental A and Experimental B blood fractions. 2. † – $p<0.05$ when comparing the control and Experimental B blood fractions.

(Fig. 11), on the fibers of which a large number of cells, in particular platelets, are detected (Fig. 11b, 12), which may in some way influence growth factors and neoangiogenesis, the concentrations of which we determined in the results of enzyme-linked immunosorbent assay (Table 2).

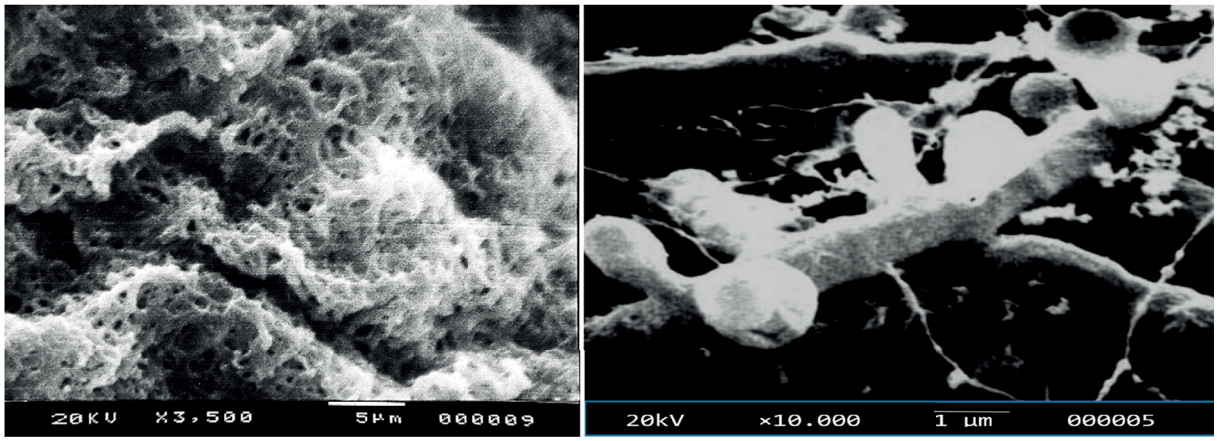
The results of the performed immunoenzymatic assay indicated a statistically significant difference between growth factor concentrations and the centrifugation protocol. Thus, when comparing VEGF-A concentrations, a statistically significant difference was observed between L-PRF, A-PRF, and I-PRF, Sticky Bone, Experimental A, and Experimental B. Specifically, the concentration of VEGF-A factor in the Experimental A and Experimental B centrifugation protocols was 2- and 3-fold higher, respectively, than the level of the same factor in the L-PRF and A-PRF protocols. However, no significant difference in VEGF-A concentration was observed between Experimental A, Experimental B, and I-PRF, Sticky bone, nor was there a significant difference between the two experimental methods.

A detailed analysis of PDGF-AA growth factor concentrations revealed a slightly different trend. Compared to the Experimental A and Experimental B centrifugation protocols, the lowest growth factor concentrations were observed in the I-PRF and Sticky Bone groups, with the latter being significantly lower than those in the experimental groups. However, a significantly higher concentration of PDGF-AA was observed in the L-PRF centrifugation mode. A comparison among the control groups indicated a significantly higher concentration of L-PRF and A-PRF compared to I-PRF and Sticky bone.

The results of the enzyme immunoassay demonstrate a clear correlation with the data from SEM. Specifically, the concentration of PDGF-AA growth factor obtained under the Experimental A and Experimental B centrifugation modes corresponds to the concentration in the L-PRF and A-PRF protocols, which also form a mechanically stable and strong fibrin matrix. This fact is confirmed by the structure of the fibrin fibers, namely the formation of a dense, tightly interwoven fibrin network that is integrated with the bone matrix. Conversely, the reduced concentration of this factor in the autologous plasma we've obtained from I-PRF and Sticky Bone corresponds to a looser and more disordered fibrin structure.

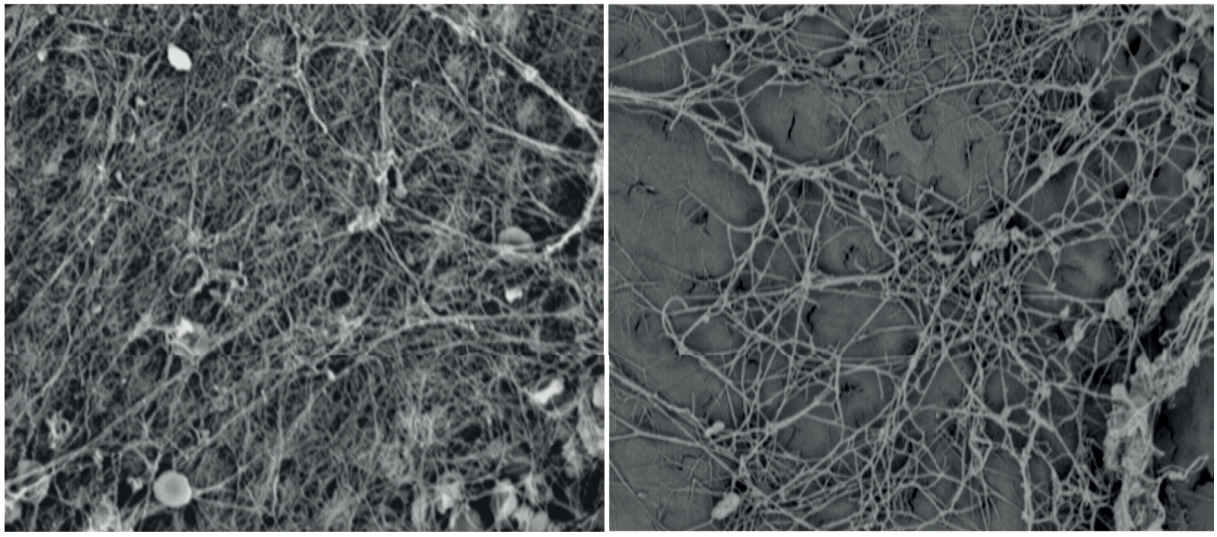
By contrast, the elevated concentration of VEGF-A factor found in Experimental A and Experimental B are consistent with the characteristics of I-PRF and Sticky Bone. However, in the latter two modes, the fibrin mesh structure is looser, and the scaffold is less mechanically stable in comparison to Experimental A and Experimental B. Consequently, in the two-step centrifugation modes Experimental A and Experimental B, it was possible to achieve an optimal balance between mechanical stability, structure, and growth factor concentration.

At the same time, in our opinion, it is imperative to acknowledge that in PRF, the expeditious release of growth factors can result in a singular peak concentration, while a prolonged release can result in a different concentration, which is important for osteointegration. The initial peak concentration of growth factors may be present in the liquid fraction of blood plasma, directly isolated from the fibrin matrix (Table 2), while another concentration of growth factors, reached over a more prolonged release period, may be directly related to the number of cells integrated into the fibrin-bone scaffold. This phenomenon may be associated with the number of platelets, which have been observed to directly influence the PDGF-AA growth factor. Additionally, the concentration of the VEGF-A growth factor may be affected by the number of other blood cells, particularly macrophages and granulocytes (neutrophils). Specifically, the number of platelets detected in I-PRF was 21,897±143.5 per 1 mm^2, which was slightly lower than 24,567±141.3 (A-PRF) per 1 mm^2. The highest number of platelets (118±6.4 in each field of view, averaging at least 36,650±180.5 platelets per 1 mm^2 of the preparation) was observed in preparations made using the Experimental A and Experimental B technologies. Similarly to platelets, the highest concentration of macrophages and



a b

Fig. 11. SEM-images of the surface of a xenograft bone following treatment with autoplasma enriched with platelet-rich plasma (a) and fixed platelets (b) during simultaneous centrifugation of bone and blood. Method: SEM; accelerating voltage 20 kV; original magnification: a×3,500, b×10,000; scale bar: a=5 µm, b=1 µm.



a b

Fig. 12. Presence of cellular elements in the interfibrillar spaces of the thrombin network. Method: SEM; accelerating voltage 20 kV; original magnification: ×1,500; scale bar: a=5 µm.

granulocytes (neutrophils), calculated as one cell per 1 µm² area, were also observed in the Experimental A (ranging from 94.64±5.41 µm² to 48.74±2.24 µm²) and Experimental B (ranging from 85.66±3.75 µm² to 52.06±2.42 µm²) protocols. Statistically significant ($p<0.05$) decreases in cell numbers were observed in the fractions obtained under the L-PRF centrifugation conditions (from 107.46±5.01 µm² to 69.46±3.30 µm²), A-PRF (from 237.19±11.54 µm² to 122.09±8.16 µm²), I-PRF (from 801.80±17.80 µm² to 194.80±4.75 µm²), and Sticky bone (from 781.96±19.96 µm² to 186.56±4.99 µm²). Therefore, considering the above indices, it can be concluded that although the concentration of VEGF-A factor is also high in the control protocols I-PRF (117.95±26.69 pg/ml) and Sticky bone (97.16±13.00 pg/ml), a more rapid peak release may predominate here, unlike Experimental A (109.22±13.35 pg/ml) and Experimental B (165.14±42.06 pg/ml). In the latter two, in addition to high concentrations of this factor, a significantly greater number of cells was also observed, which may result in a more prolonged release of this factor.

The optimal organization of the fibrous-bone structure of such a fibrin-bone matrix obtained using the Experimental A and Experimental B protocols, combined with the optimal concentration of inductive components, in our opinion, will contribute to better mechanical stability of the scaffold we obtained and effective osteoconduction and osteoinduction when this osteofibrin mass is introduced into the surgical field, for example during sinus lifting. In contrast, the use of the standard I-PRF and Sticky Bone protocols resulted in the formation of a less stable scaffold, although they yielded high concentrations of VEGF-A

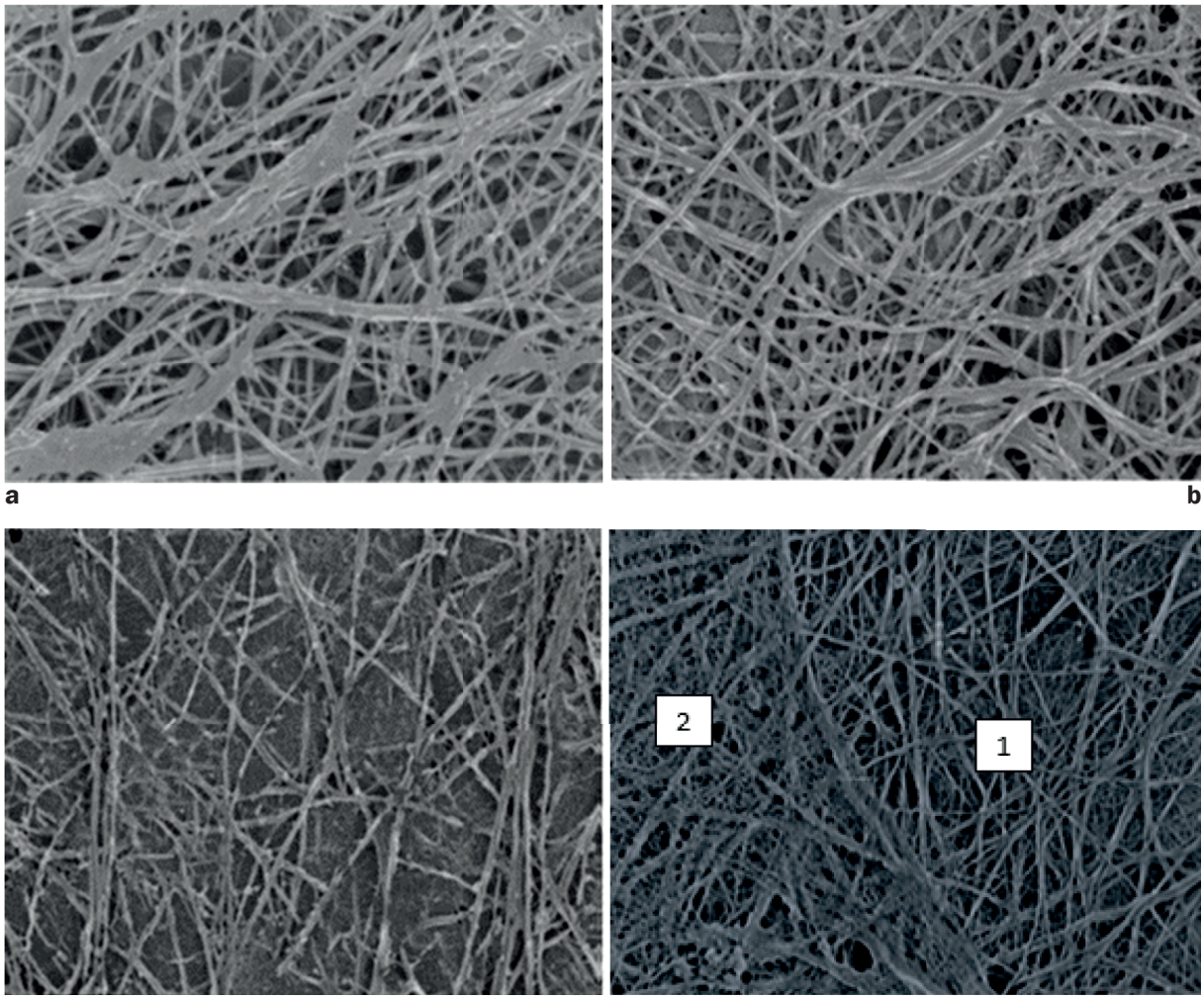


Fig. 13. General view of the fibrin mesh obtained under different centrifugation conditions. SEM-micrographs show four types of microfibrillar structures: (a) – corresponds to type A-PRF, (b) – corresponds to type L-PRF, (c) – corresponds to type I-PRF and Sticky bone, (d) – corresponds to the Experimental A and Experimental B modes (1-fibrous structure; 2-fine fibrin network covering the fibrous structure). Method: SEM; accelerating voltage 20 kV; original magnification: a×3,500, b×10,000; scale bar: a=5 μm, b=1 μm.

factor. It is confirmed by microscopic analysis, in which the surface appeared not as an organized mesh but as loose, fine, needle-like structures (Fig. 10e).

The performed microscopic analysis enabled the identification of to four major types of fibrous fibrin network structures depending on the centrifugation protocols (Fig. 13).

The analysis of the fibrin matrix structure (Fig. 13 a, b) revealed the formation of a coarse-fibrous scaffold with uneven fibrin fiber thickness, which was characteristic of the A-PRF and L-PRF centrifugation protocols. In contrast, a looser and more disordered structure (Fig. 13c) corresponded to the I-PRF and Sticky bone centrifugation modes, which correlated with the ratios of the liquid plasma fraction to the gel-like polymerized fibrin fraction (Table 1). It was under these centrifugation conditions that the smallest area of organized fibrin was observed, with the liquid plasma fraction predominating. Although in the Experimental A and Experimental B protocols (thinner fibrin fibers predominated in the fibrin structure, unlike in A-PRF and L-PRF), their organization consisted of a very fine, dense fibrin network, which was not observed under any centrifugation mode (Fig. 13d). It was also observed that the same organized fine fibrin network was present in the micropores of the bone matrix (Fig. 8c).

Discussion

The results of our studies suggest that the hybrid fibrin fiber structure we've obtained using Protocols Experimental A and Experimental B (Fig. 13d) may, in our opinion, play an important role in the formation of bone tissue in the implantation site of such a fibrin-bone matrix. The specific type of hybrid

microstructure we obtained, which combined both thicker fibers and a fine, dense network, may be associated with the two-stage, variable-speed centrifugation protocol (Experimental A and Experimental B). The low speed during the initial centrifugation stage, in conjunction with an extended duration, may have facilitated the formation of a fine fibrin mesh and thicker fibers, whereas the higher speed over a short period during the second stage may have formed thicker fibers and influenced their ultimate remodeling.

Regarding the influence of other factors on the structure of the fibrin network, the answer may lie in their direct effect on the mechanism of fiber formation itself. Consequently, during clot formation, fibrinogen is converted into thrombin resulting in the formation of fibrin monomers. These monomers then assemble into protofibrils, which subsequently combine to form fibrils. The fibrils, in turn, form fibers that constitute the spatial network itself, within which fiber cross-linking occurs via factor XIIIa. Overall, this is a highly mechanosensitive process (milliseconds-seconds, nanoscale). Therefore, it logically follows that several factors during the centrifugation process itself can influence this phenomenon, namely speed, time, centrifugal force, and a certain range of vibration. The latter can lead to disorganization of polymerization (chaotic collisions of monomers) and disruption of linear fibril growth, which ultimately affects fiber thickness and the breakdown of initial (weak) bonds. In the early stages, hydrogen and hydrophobic interactions predominate. These bonds break easily even under minor mechanical disturbances, resulting in a less ordered network. Disruption to cross-linking can also occur due to factor XIIIa, since the cross-linking requires stable fiber geometry, whereas vibration causes constant micro-displacement, resulting in a reduced number of covalent cross-links. This can lead to lower mechanical strength, a factor that is particularly critical for the integrated bone matrix. Another factor to be considered is the degree of fibrin adhesion to the surface of the bone matrix granules, since fibrin must penetrate the pores and "adhere" to the matrix, while vibration has been shown to reduce contact time and may disrupt the "anchoring" of the fibers, potentially resulting in a mechanically unstable fibrin-bone matrix. As indicated by other authors, the potential impact of vibration on the fibrin network state has been a subject of research[14]. Specifically, Dohan Ehrenfest et al., in their comparative analysis of different operating modes on various centrifuges, found that vibration affected the structure of fibrin fibers and reduced their thickness; however, vibration did not completely destroy the formed network[14].

Consequently, mechanical vibration does not directly disrupt the molecular bonds of fibrin; however, it significantly alters the kinetics of its polymerization, thereby disrupting the formation of protofibrils and their spatial organization. This phenomenon may be accompanied by a decrease in the density of the network due to a reduction in the thickness of fibrin fibers, insufficient covalent cross-linking, and a possible deterioration in fibrin adhesion to the surface of bone-plastic material granules; these factors collectively reduce the biomechanical stability of the formed scaffold. In another option, the properties of fibrin may change during centrifugation; when, with minimal vibration or none at all, in the presence of densely packed bone matrix granules, which may also influence fibrin polymerization, thin and long fibers with high density, good cross-linking (factor XIIIa), and deep integration into the bone matrix with improved biomechanical strength may form.

Centrifugal force, velocity, and a specific range of vibration over a certain period of time can, in some cases, actually remodel the fiber structure in the desired direction, which is also consistent with the model of two-stage and simultaneous centrifugation of blood with fine bone granules (Experimental A and Experimental B). During the simultaneous centrifugation of blood and bone-plastic material, the vibration transmitted to the material granules can locally influence the organization of fibrin fibers around individual granules, forming a fine mesh of fibrin fibers on the surface of the bone matrix and within its microscopic pores (Fig. 8 and Fig. 10 a, b, c, d). On the one hand, this may provide additional mechanical stability to the bone matrix granules themselves within the fibrin scaffold. Conversely, the presence of such a fine fibrin mesh within the micropores (Fig. 8c) may potentially facilitate the deposition of protein components that are essential for bone formation. This will significantly increase the contact area between the newly formed bone tissue and the matrix, thereby providing additional mechanical retention of the implanted bone matrix with the newly formed bone tissue. There was performed an analysis of the structure and organization of fibrin in combination with bone under standard processing protocols using I-PRF and Sticky Bone (Fig. 10e), and after simultaneous centrifugation of bone material granules and blood it revealed the significantly better organization and integration of fibrils with the bone matrix in the latter approach (Fig. 8 and Fig. 10a, b, c, d).

Another factor that influenced the formation of the fibrin mesh, in our opinion, could be due to the presence of granules of bone-plastic material during centrifugation, which may have acted as a catalyst for

the formation of a significantly larger amount of polymerized fibrin. The formation of a greater amount of polymerized fibrin could also have been influenced by the presence of a Ti-6Al-4V titanium alloy filter, which is used during the simultaneous centrifugation of bone-plastic material and blood. This fact is confirmed by the negligible quantity of liquid plasma (0.28±0.014 mL) that was formed immediately after centrifugation, in contrast to conventional PRF (1.54±0.040 mL). The influence of titanium on the fibrin structure is also noted by Mustafa et al[15], who demonstrated that the fibrin matrix exhibited a denser network and a more organized structure during centrifugation, in contrast to centrifugation in a glass tube. The authors attribute this peculiarity is associated with the better biocompatibility and hemocompatibility of titanium in comparison to glass.

Our comprehensive review of the scientific literature also indicated the use of platelet-rich fibrin to improve the outcomes of dental implantation, particularly to enhance the stability of dental implants[5]. Consequently, the further refinement of technologies for producing fibrin scaffolds with programmed osteoconductive and osteoinductive properties represents a distinct and very important area of scientific research in this field. In particular, consistent with the findings of other researchers[16], a discernible correlation was identified between the centrifugation speed, the quantity of cellular components, and the configuration of the fibrin mesh. The fibrin-bone scaffold obtained under the corresponding two-stage centrifugation regimes (Experimental A and Experimental B), is in our opinion, fits the optimal model of an osteoconductive and osteoinductive matrix. The initial stage of low-speed centrifugation enables the isolation of the required amount of VEGF-A factor for the rapid release, a feature also observed in the I-PRF and Sticky Bone protocols. By contrast, the second stage, which is performed at a higher velocity, in our opinion, affects the quantity and quality of polymerized fibrin, which retains a significantly larger number of cells for a more prolonged release of VEGF-A and PDGF-AA growth factors. It has been established that different modes of fibrin-bone matrix preparation result in different structures of the fibrin scaffold and different concentrations of growth factors. This is attributable to the varying content of platelets and other blood cells in the loops of the fibrin mesh formed on the surface of the bone matrix under different centrifugation conditions, which is consistent with the findings of other authors[1,2,4,16]. Such a difference in microstructure, in our opinion, serves as the morphological basis for explaining the effective osseointegration of the fibrin-bone scaffold formed using the authors' method upon implantation into a bone defect as evidenced in our previous studies[17], and confirms the feasibility of this modification method prior to implantation into autogenous bone. The micro- and nanofibrous structure of the scaffold obtained under the two-stage centrifugation regimes (Experimental A and Experimental B), combined with a high concentration of growth factors, is, in this study, deemed to be the optimal solution for the bone integration process. The method of forming a fibrin-bone scaffold enriched with growth factors is a type of subtractive method.

Conclusions

When bone-plastic material and the patient's blood are subjected to simultaneous centrifugation, in accordance with the experimental protocols that have been developed in our study, a fine fibrillar structure forms not only on the surface of the bone matrix, but also within its porous structure. The experimental two-stage centrifugation regimen developed combines mechanical stability, due to the organized fibrous structure of fibrin, with inductive properties, due to the high concentration of growth factors and a greater number of cells in the resulting scaffold.

Centrifugation regimes significantly influence the morphology of the fibers themselves, the concentrations of growth factors, and the number of cells in the fibrin matrix. The interrelationship between the presence of a filter made of biocompatible titanium Ti –6Al-4V and a small volume of the liquid plasma phase formed immediately after centrifugation, creates optimal conditions for the formation of a fibrin-bone scaffold with a higher concentration of growth factors and improved mechanical stability of the fibrin scaffold.

Author Contributions:

Conceptualization, A.V.P., N.Y.K.; methodology, N.Y.K., I.R.Y.; software, A.V.P.; validation, M.M.R.; formal analysis, A.V.P.; investigation, A.I.C., A.V.P.; resources, M.M.R.; data curation, M.M.R. and A.V.P.; writing–original draft preparation, A.I.C.; writing–review and editing, A.V.P.; visualization, A.I.C.; supervision, M.M.R.; project administration, M.M.R. All the authors have read and agreed with the final version of the article.

Compliance with Ethics Requirements:

"The authors declare no conflict of interest regarding this article"

"The authors declare that all the procedures and experiments of this study respect the ethical standards in the Helsinki Declaration of 1975, as revised in 2008(5), as

well as the national law. Informed consent was obtained from all the patients included in the study"

"No funding for this study"

Acknowledgements:

We express our sincere gratitude to Associate Professor Serhiy L. POPEL, Vasyl Stefanyk Carpathian National University, and Yuriy R. DATSYUK, Assistant, The Department of Mineral Geology and Geophysics, Ivan Franko National University of Lviv, for assistance in the scanning electron microscopy analysis.

References

1. Charalambides C, Beer M, Cobb AG. Poor results after augmenting autograft with xenograft (Surgibone) in hip revision surgery. *Acta Orthop.* 2015;3(98):34-40. DOI: 10.1080/17453670510041547.
2. Levai JP, Bringer O, Descamps S, Boisgard S. Xenograft-related complications after filling valgus open wedge tibial osteotomy defects. *Rev Chir Orthop Reparatrice Appar Mot.* 2018;89(8):707-711.
3. Kubosch EJ, Bernstein A, Wolf L, Fretwurst T. Clinical trial and in-vitro study comparing the efficacy of treating bony lesions with allografts. *J Oral Maxillofac Surg.* 2017;55(8):822-829. DOI: 10.1186/s12891-016-0930-1.
4. Burnouf T, Goubran HA, Chou M-L. Platelet microparticles: Detection and assessment of their paradoxical functional roles in disease and regenerative medicine. *Blood Rev.* 2023; 2(83): 155-66. https://doi.org/10.1186/s12929-023-00972-w
5. Vandson SM, Rodrigo AR, José MB L do A, Angelica CP, Lilian AP, Caio VGR-T. The use platelet rich fibrin in dental implants: A literature review. *Trends in Transplant.* 2018; 11(2): 1-3. doi: 10.15761/TiT.1000253
6. Crisci A, Lombardi D, Serra E, Lombardi G, Cardillo F, Crisci M. Standardized protocol proposed for clinical use of L-PRF and the use of L-PRF Wound Box®. *J Unexplored Med Data.* 2017; 2: 77-87. DOI:10.20517/2572-8180.2017.17 [in English]
7. Kubesch A, Barbeck M, Al-Maawi S, et al. A low-speed centrifugation concept leads to cell accumulation and vascularization of solid platelet-rich fibrin: An experimental study in vivo. *Platelets.* 2019; 30(3): 329-340. doi: 10.1080/09537104.2018.1445835. [in English]
8. Lee HM, Shen EC, Shen JT, Fu E, Chiu HC, Hsia YJ. Tensile strength, growth factor content and proliferation activities for two platelet concentrates of platelet-rich fibrin and concentrated growth factor. *J. Dent. Sci.* 2020; 15(2):141-146. doi: 10.1016/j.jds.2020.03.011. [in English].
9. Li W, Sigley J, Pieters M, et al. Fibrin fiber stiffness is strongly affected by fiber diameter, but not by fibrinogen glycation. *Biophys. J.* 2016; 110(6): 1400–1410. doi: 10.1016/j.bpj.2016.02.021. [in English]
10. McLellan J, Plevin S. Temporal release of growth factors from platelet- rich fibrin (PRF) and platelet-rich plasma (PRP) in the horse: a comparative in vitro analysis. *International Journal of Applied Research in Veterinary Medicine.* 2014;12(1):48-57. [in English]
11. Kim BJ, Kwon TK, Baek HS, et al. A comparative study of the effectiveness of sinus bone grafting with recombinant human bone morphogenetic protein 2-coated tricalcium phosphate and platelet-rich fibrin-mixed tricalcium phosphate in rabbits. *Oral Surg Oral Med Oral Pathol Oral Radiol.* 2012;113(5):583-92. doi: 10.1016/j.tripleo.2011.04.029. [in English].
12. De Almeida NCPM, Dos Santos NBM, Completo AMG, De Oliveira FGV. Tensile strength assay comparing the resistance between two different autologous platelet concentrates (leucocyte-platelet rich fibrin versus advanced- platelet rich fibrin): A pilot study. *Int. J. Implant Dent.* 2021; 7(1):1. doi: 10.1186/s40729-020-00284-w.
13. El Bagdadi K, Kubesch A, Yu X, et al. Reduction of relative centrifugal forces increases growth factor release within solid platelet- rich fibrin (PRF)-based matrices: a proof of concept of LSCC (low speed centrifugation concept). *European Journal of Trauma and Emergency Surgery.* 2019;45(3):467-79.
14. Dohan Ehrenfest DM, Pinto NR, Pereda A, et al. The impact of the centrifuge characteristics and centrifugation protocols on the cells, growth factors, and fibrin architecture of a leukocyte- and platelet-rich fibrin (L-PRF) clot and membrane. *Platelets.* 2018;29:171–184. doi: 10.1080/09537104.2017.1293812.
15. Mustafa T, Hakan Ö, Zafer K, et al. A novel platelet concentrate: Titanium-prepared platelet-rich fibrin. *BioMed Research International.* 2014, Article ID 209548. http://dx.doi.org/10.1155/2014/209548
16. Oranit B, Wutigri N, Supatra S. The impact of centrifugation devices and collection tubes on fibrin characteristics and growth factor release under high and low-speed protocols. *Dent J (Basel).* 2025;13(10):476. doi: 10.3390/dj13100476.
17. Yevchuk YuI, Rozhko MM, Pantus AV, Yarmoshuk IR, Pantus PV. Analysis of the clinical effectiveness of using the created combined fibrin-bone scaffold for the reconstruction of bone tissue defects of the jaws. *Georgian Medical News.* 2024; 7-8 (352-353):6-13.